scientific reports

Check for updates

OPEN

Elucidating common biomarkers and pathways of osteoporosis and aortic valve calcification: insights into new therapeutic targets

Yujian Lan[1,2,5], Qingping Peng[1,2,5], Jianlin Shen[3,4]✉ & Huan Liu[2]✉

Background: Osteoporosis and aortic valve calcification, prevalent in the elderly, have unclear common mechanisms. This study aims to uncover them through bioinformatics analysis. Methods: Microarray data from GEO was analyzed for osteoporosis and aortic valve calcification. Differential expression analysis identified co-expressed genes. SVM-RFE and random forest selected key genes. GO and KEGG enrichment analyses were performed. Immunoinfiltration and GSEA analyses were subsequently performed. NetworkAnalyst analyzed microRNAs/TFs. HERB predicted drugs, and molecular docking assessed targeting potential. Results: Thirteen genes linked to osteoporosis and aortic valve calcification were identified. TNFSF11, KYNU, and HLA-DMB emerged as key genes. miRNAs, TFs, and drug predictions offered therapeutic insights. Molecular docking suggested 17-beta-estradiol and vitamin D3 as potential treatments. Conclusion: The study clarifies shared mechanisms of osteoporosis and aortic valve calcification, identifies biomarkers, and highlights TNFSF11, KYNU, and HLA-DMB. It also suggests 17-beta-estradiol and vitamin D3 as potential effective treatments.

Keywords Osteoporosis, Aortic valve calcification, Bioinformatics analysis, Machine learning, Molecular mechanisms

Abbreviations

GEO	Gene Expression Omnibus
GO	Gene Ontology
KEGG	Kyoto Encyclopedia of Genes and Genomes
TFs	Transcription factors
GSEA	Gene Set Enrichment Analysis
AVC	Aortic valve calcification
AVS	Aortic valve stenosis
OP	Osteoporosis
LIMMA	Linear Model for Microarrays
DEGs	Differentially expressed genes
PPI	Protein-protein interactions
BP	Biological processes
MF	Molecular functions
CC	Cellular components
RF	Random forest
SVM-RFE	Support vector machines recursive feature elimination
ROC	Receiver operating characteristic curve
AUC	Area under the curve
TNFSF11	Tumor Necrosis Factor Ligand Superfamily Member 11
Tregs	T cells regulatory

[1]School of Integrated Traditional Chinese and Western Medicine, Southwest Medical University, Luzhou 646000, Sichuan, China. [2]Department of Orthopaedics, The Affiliated Traditional Chinese Medicine Hospital, Southwest Medical University, Luzhou 646000, Sichuan, China. [3]Department of Orthopaedics, Affiliated Hospital of Putian University, Putian 351100, Fujian, China. [4]Central Laboratory, Affiliated Hospital of Putian University, Putian 351100, Fujian, China. [5]These authors contributed equally to this work: Yujian Lan and Qingping Peng. ✉email: shenjianlinchina@126.com; 20016040@163.com

RANKL	Receptor Activator of Nuclear Factor κ-B Ligand
TNF-α	Tumor necrosis factor-alpha
LDL	Low-density lipoprotein
RMSE	Root mean square error
AGEs	Advanced glycation end-products
RAGE	AGE receptor
VSMCs	Vascular smooth muscle cells
Erα	Estrogen receptor alpha
GWAS	Genome-Wide Association Study
SNPs	Single nucleotide polymorphisms

Aortic valve calcification (AVC) stands out as a highly prevalent valvular condition and is widely regarded as the primary etiology of aortic valve stenosis (AVS), a condition that can culminate in severe cardiac complications including heart failure and sudden cardiac death[1,2]. AVC is typified by a gradual fibrocalcific remodeling process affecting the valve leaflets[3]. Currently, there are no practical methods available to prevent the onset or impede the progression of AVC. Surgical intervention or transcatheter aortic valve replacement represents the sole efficacious treatment option once the disease has advanced to a critical stage[4]. AVC exhibits a higher prevalence among the elderly population and was historically perceived as a degenerative disease with passive characteristics. There exists an imperative to deepen our comprehension of the pathogenesis of AVC and to identify viable therapeutic targets.

Osteoporosis (OP) is a systemic skeletal disorder marked by diminished bone density, heightened bone fragility, and increased vulnerability to fractures[5]. The process of bone resorption is insidious and does not manifest overt symptoms directly. Pain and skeletal deformities manifest when the local bone strength fails to withstand the imposed mechanical stress[6]. The likelihood of fractures is correspondingly elevated[7]. Reports indicate that over 200 million individuals globally are impacted by OP[8]. Consequently, mitigating the prevalence of OP and elucidating its pathogenesis have emerged as pressing public health imperatives.

There is a mounting body of evidence indicating the association between diseases of the vascular system and bone metabolism. Scholars have postulated the concept of a bone-vascular axis to probe the correlation between these systems, suggesting that disturbances in the bone-vascular axis due to metabolic abnormalities could lead to the simultaneous occurrence of vascular and skeletal diseases[9]. OP and AVC are prevalent skeletal and vascular disorders, also representing chronic systemic ailments and significant global public health challenges[10]. Several epidemiologic studies have demonstrated a correlation between cardiovascular calcification and OP[11]. The coexistence of AVC and OP in patients suggests that they share common causative factors (e.g., hyperlipidemia)[12]. And, there is growing evidence of a potential link between OP and AVC[13]. While a consensus on the precise cellular and molecular basis of the high co-morbidity between OP and AVC remains elusive, studies have demonstrated the sharing of common risk factors, pathogenic elements, genetic factors, and a causal relationship between the two[14]. Furthermore, research has revealed a direct link between the extent of cardiovascular calcification and bone mineral damage[15]. Multiple pathophysiological mechanisms have been recognized, including factors such as inflammatory cytokines, products of lipid oxidation, and deficiencies in vitamins D and K[2,16,17]. Cytokines involved in inflammation, such as tumor necrosis factor-alpha (TNF-α) and interleukins IL-1, IL-6, and IL-17, alongside various chemokines, have been linked to atherosclerosis, heightened rates of cardiovascular morbidity and mortality, and increased bone turnover[18]. Dyslipidemia, characterized by elevated levels of total cholesterol, triglycerides, and low-density lipoprotein (LDL) cholesterol, is believed to play a role in the advancement of atherosclerosis, while also influencing bone metabolism[12,19]. Evidence suggests that factors promoting vascular cell calcification, like modified lipoproteins, can negatively impact the calcification processes of osteoclasts within the skeletal system. In a similar vein, inflammatory cytokines such as TNF-α and IL-1, which encourage vascular calcification, also promote bone resorption. Collectively, these findings indicate that OP inhibitors might either mitigate or exacerbate vascular calcification[20].

Consequently, a deeper exploration of prevalent biomarkers and innovative pathways related to AVC and OP within this study will aid in the advancement of prevention strategies that serve dual purposes. Various bioinformatics analyses were employed to uncover key biomarkers and biological roles, thereby offering valuable insights into potential innovative therapeutic targets. Furthermore, our research involved the prediction of potential small molecule drugs that target both OP and AVC diseases, presenting novel opportunities for future follow-on treatments of cardiovascular calcification diseases and bone metabolic disorders.

Methodology

Data collection

Figure 1 depicts the flowchart of this study. Datasets related to OP and AVC were screened in the Gene Expression Database (GEO) (http://www.ncbi.nlm.nih.gov/geo/). GSE51472 includes gene expression profiles of 5 calcified samples and 5 normal samples (Table 1), in addition to GSE56815, which provides a complete dataset including gene expression profiles of blood mononuclear cells from 40 women with high and 40 women with low bone density (Table 2).

Differential gene expression analysis

We compared the data sets for OP using the Linear Model for Microarrays (LIMMA) package in R (version 4.1.2). Differentially expressed genes (DEGs) were identified between the disease and control groups. For AVC, the threshold for DEGs was set at a P value of <0.05 and $|\log2FC|\geq1.5$ (fold change). In the case of OP, DEGs were identified using a P value adjusted to <0.05. Subsequently, volcano plots were utilized to present the results of the analysis of variance for each group. The intersections were determined based on the differential

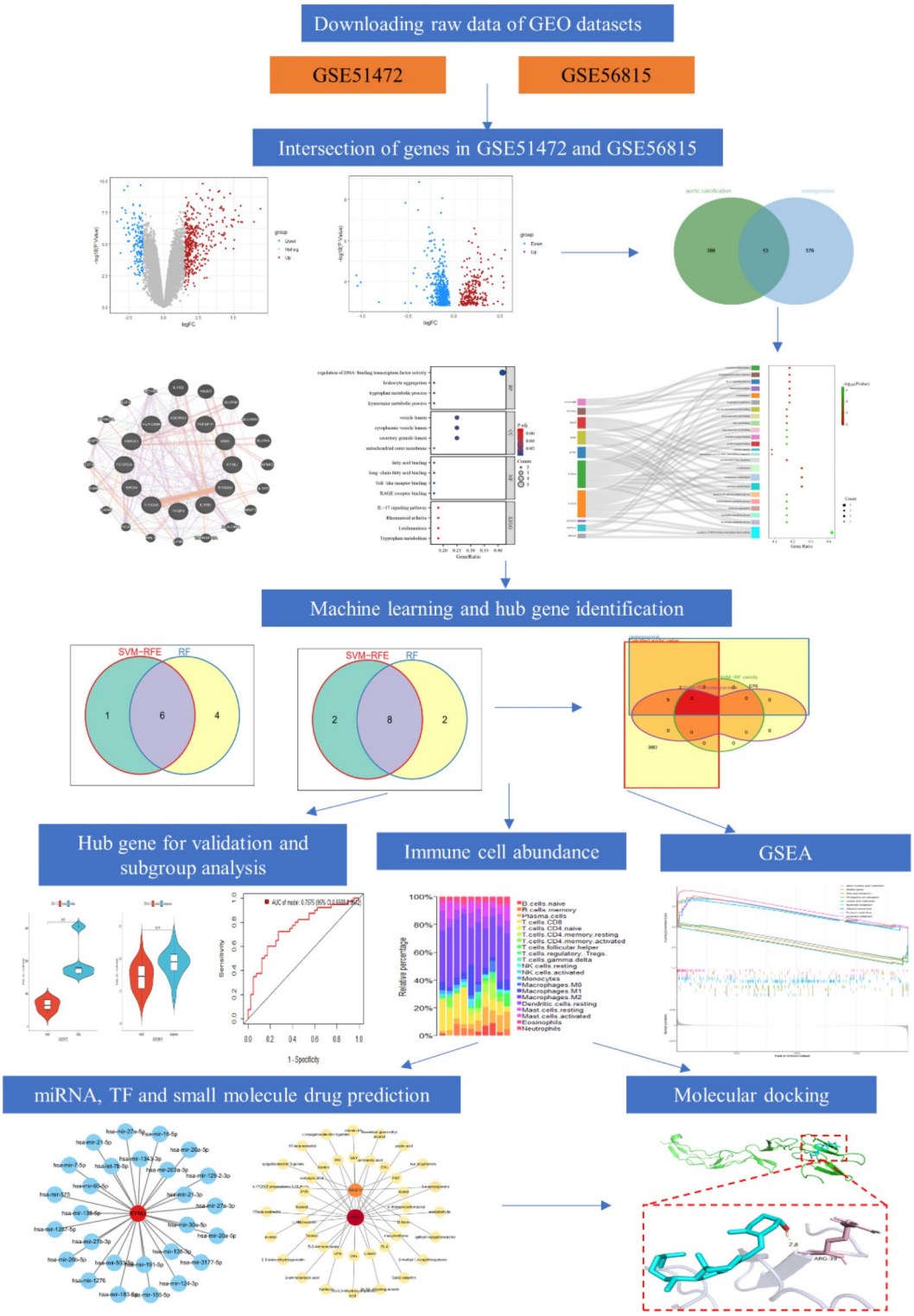

Fig. 1. Study flowchart of the whole procedures.

expression results of the two diseases and displayed in Venn diagrams. Heatmaps illustrating the expression levels of the intersected genes in both diseases were then generated, with blue representing low expression and red representing high expression[21].

PPI network construction and enrichment analysis of shared genes for AVC and OP

To further explore the interrelationships among the shared genes, a protein-protein interactions (PPI) network was constructed using GeneMANIA[22]. The potential functions of the shared genes were identified using the

GSE51472	Control	Disease
N. of patients	5	5
Sex	Male (100%)	Male (100%)
Age (yrs)	43.8 ± 18.4 (31–69)	56.8 ± 9.9 (45–72)
Diagnosis	Normal aortic valve	AVC

Table 1. Demographic data for AVC dataset GSE51472.

GSE56815		Control	Disease
N. of patients	Premenopausal	20	20
	Postmenopausal	20	20
Sex		Females (100%)	Females (100%)
Age (yrs)		49.4 (8.1)	50.0 (7.9)
Diagnosis		High bone mineral density (BMD)	Low BMD (OP)

Table 2. Demographic data for OP dataset GSE56815.

"org.Hs.eg.db" in R software, along with the "ggplot2," "clusterProfiler,"[23]and "enrichment" software packages, for analyzing the Gene Ontology (GO) and Kyoto Encyclopedia of Genes and Genomes (KEGG)[24] pathways. Subsequently, Gene Ontology (GO) analyses were conducted to unveil shared gene-associated biological processes (BP), molecular functions (MF), and cellular components (CC). Additionally, Kyoto Encyclopedia of Genes and Genomes (KEGG) analysis was performed to identify enriched signaling pathways associated with potential targets. The statistical significance of the results was assessed based on a p-value of < 0.05.

Feature selection by two well-established machine learning algorithms

Two established machine learning algorithms, namely SVM-RFE (Support Vector Machine-Recursive Feature Elimination) and RF (Random Forest), were employed in this study. To ensure the reproducibility of the results, a seed value of 12,345 was set for both disease groups when running the algorithms. Initially, the 13 shared genes obtained earlier were input into the SVM-RFE algorithm for each disease group to eliminate redundant features. SVM modeling was conducted utilizing the "e1071" and "MSVM-RFE" software packages, with SVM-RFE employing sequential backward feature elimination to identify the most significant genes. All 13 shared genes were included in the SVM model. The results obtained from SVM-RFE were visualized and validated through 10-fold cross-validation[21].

Finally, Random Forest was employed to classify the significant genes using the R package "randomForest". Using a decision tree algorithm, the random forest analysis determined which variables were most important. Thanks to this algorithm, we were able to filter shared genes to find disease signature genes. Our first step was to construct a Random Forest model using 500 trees from the discovery cohort and determine the optimal number of trees using cross-validation errors. We then ranked the genes by importance and mapped the 10 most important genes[21].

Following the screening of both algorithms, the intersection of their respective results was determined. The Venn diagram revealed 6 common genes in the AVC group and 8 common genes in the OP group. Furthermore, by intersecting the previously identified common genes, we isolated 3 genes as potential disease diagnostic targets. ROC curves were generated utilizing the "pROC" package and visualized with "ggplot2" to evaluate the precision of the two diagnostic genes in the discovery cohort.

Hub gene expression and ROC evaluation

Hub gene expression profiles were initially evaluated in the GSE51472 and GSE56815 datasets, and then ROC curves were constructed using the "pROC" package and displayed using "ggplot2" to evaluate the diagnostic value of the hub gene for OP, respectively. The diagnostic value of hub gene for OP was evaluated separately. The AUC values and their corresponding 95% confidence intervals were calculated to differentiate the disease group from the control group, and AUC values above 0.7 were considered to be significantly different[25].

Immune cell abundance

CIBERSORT is a powerful technique for determining the relative abundance of immune cells for analysis of each disease sample. The algorithm utilizes gene expression data to accurately estimate the composition of immune cells. Comparative analysis of immune cell infiltration between diseased and normal samples is performed using CIBERSORT to determine the relative level of immune cells. The CIBERSORT algorithm resolves immune cell composition by back-convolution based on gene expression data. Using CIBERSORT and 1000 iterations, we quantified 22 immune cell species based on the LM22 gene signature. The 22 immune cell types and CIBERSORT metrics such as CIBERSORT p-values, Pearson correlation coefficients, and root mean square error (RMSE) were quantified for each sample[26]. R packages "corrplot" and "ggplot2" were used to visualize the results[27].

Implementation of GSEA for hub gene

After obtaining the hub genes, we used the 'clusterProfiler' software package to perform cluster enrichment analysis (GSEA) of the hub genes in the two disease groups. Using GSEA, we investigated the biological signalling pathways of the hub genes in the disease groups, and Enrichplot was used to display the top 5 activation and inhibition pathways of each gene in both disease groups[28].

Construction of TF-gene, miRNA-gene and small molecule drug prediction co-expression networks

NetworkAnalyst 3.0[29] is a powerful visualization and analysis tool for in-depth gene expression profiling, which we used to input machine learning screened hub genes into the site.The corresponding TF targets derived from the JASPAR TF binding The corresponding TF targets were derived from the JASPAR TF binding site profile database. The corresponding miRNAs were collected from miRTarBase, a comprehensive and experimentally validated miRNA gene interaction data. Then the prediction results were imported into cytoscape software to construct TF-gene, miRNA-gene network diagrams, respectively. Subsequently, the small molecule compounds corresponding to the characterized genes were identified based on the database HERB (HERB), and the small molecule compound data were collected from multiple databases, and then the network diagrams were plotted with cytoscape.

Molecular docking

Initially, we retrieved the PDB structure file of the target hub proteins from the PDB database[30](https://www.rcsb.org/, accessed on 29 September 2024) and employed PyMOL to eliminate solvent and water molecules[31]. Subsequently, we utilized AutoDockTools 4.2.6 to add hydrogens, compute charges, and convert the proteins to the PDBQT format[32]. The 3D structure file of curcumin was obtained from PubChem[33] and converted to a pdb file using Open Babel GUI[34]. The resultant curcumin pdb file was imported into AutoDockTools, where hydrogens were added, charges were computed, it was designated as the docking ligand, and its Torsional Trees were set. This was then exported in PDBQT format. By analyzing the binding site of the target hub proteins, we identified the corresponding docking active pocket. We utilized AutoGrid to set the Grid Box and executed the process. AutoDock was configured with the Genetic Algorithm (Number of GA Runs = 50), default Docking Parameters, and executed for docking validation. Finally, PyMOL was used to visualize the docking results.

Results

Identification of DEGs, genes shared by AVC and OP

The LIMMA package was used to characterize the DEGs between AVC and OP. In the case of AVC, a total of 393 DEGs (P value <0.05, $|\log2\ FC|\geq1.5$) were identified, comprising 283 up-regulated and 110 down-regulated genes. Regarding OP, a total of 589 DEGs (P value <0.05) were observed, consisting of 205 upregulated genes and 384 downregulated genes. Volcano maps illustrating the DEGs for AVC (Fig. 2A) and OP (Fig. 2B) were generated. Subsequently, the intersection of the DEGs from both conditions revealed 13 shared genes (HMOX1, FCGR2A, TFDP2, TNFSF11, ADORA3, GUSBP11, IL1RN, HLA-DMB, KYNU, KMO, SRGN, S100A8, and S100A9) (Fig. 2C). These shared genes potentially contribute to the pathogenesis and progression of both AVC and OP, as depicted in the heat maps (Fig. 2D, E). The shared genes linked to AVC and OP potentially contribute to the pathogenesis and progression of these conditions.

Gene enrichment analysis of shared genes for AVC and OP

The PPI networks of the candidate genes were constructed utilizing the Gene-MANIA database (Fig. 3A) and subjected to functional analysis through GO, KEGG to elucidate potential mechanisms of action. The results showed that GO enrichment regulated the activity of DNA-binding transcription factors, leukocyte aggregation, tryptophan metabolic process, kynurenine metabolic process (BP); fatty acid binding, long-chain fatty acid binding, Toll-like receptor binding, and RAGE receptor binding (MF); vesicle lumen, cytoplasmic vesicle lumen, secretory granule lumen, mitochondrial outer membrane (CC). In addition, these genes showed significant enrichment in KEGG pathways, including the 1 L-17 signaling pathway, Rheumatoid arthritis, Leishmaniasis, Tryptophan metabolism (Fig. 3B C).

Identification of potential shared hub genes based on machine learning algorithms

To identify the hub gene targets with the most influential eigenvalues for distinguishing between disease and control groups, two distinct algorithms (SVM-RFE and Random Forest) were employed using the previously mentioned 13 shared genes. Within the AVC group, the SVM algorithm detected 7 genes (Fig. 4A). Subsequently, the aforementioned 13 genes were inputted into the Random Forest (RF) classifier, revealing the top 10 genes based on their importance ranking (Fig. 4B). Furthermore, through the intersection of these two algorithms, 6 common biomarkers (ADORA3, FCGR2A, KMO, TNFSF11, KYNU, HLA-DMB) were identified in the AVC group (Fig. 4C). Likewise, in the OP group, the Support Vector Machine (SVM) algorithm pinpointed 10 genes (Fig. 4D) and highlighted the top 10 genes based on their importance ranking. Subsequently, through the convergence of these two algorithms, 8 common biomarkers in the OP group were identified (HMOX1, S100A8, SRGN, TNFSF11, GUSBP11, KYNU, HLA-DMB, TFDP2) (Fig. 4F).

Diagnostic value of diagnostic center biomarkers

To enhance our comprehension of the association between AVC and OP, we leveraged the overlap of machine learning outcomes from both the AVC and OP cohorts, identifying three common diagnostic genes: TNFSF11, KYNU, and HLA-DMB (Fig. 5A). The predictive and discriminative capabilities of the shared diagnostic genes were evaluated through an analysis of their expression profiles. Initially, we scrutinized the expression levels of the

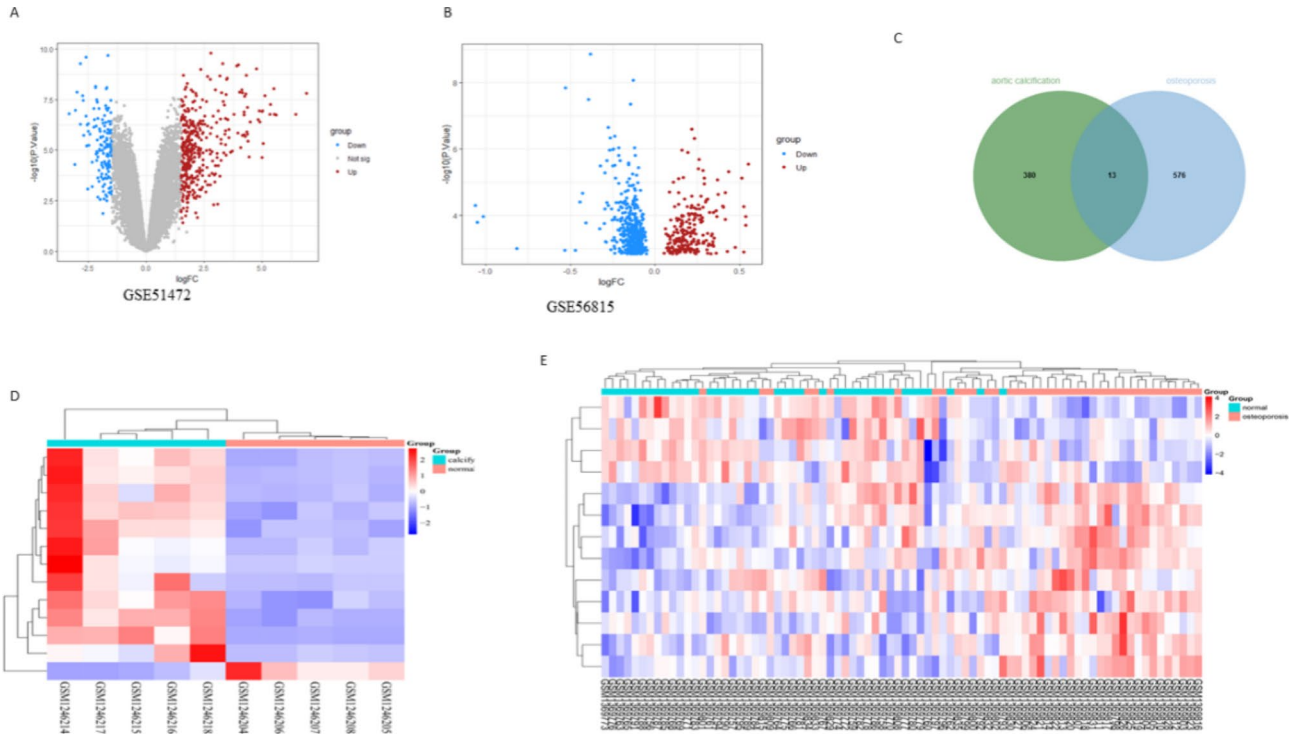

Fig. 2. Identification of DEGs and common genes in the OP GSE56815 and AVC GSE51472 datasets. A. Volcano plots of DEGs in AVC.B. Volcano plots of DEGs in OP.C. Wayne plots of intersecting genes of DEGs of the two diseases in OP and AVC.D. Heatmaps of common genes of the two diseases in the AVC dataset. E. Heatmaps of common genes of the two diseases in the OP dataset.

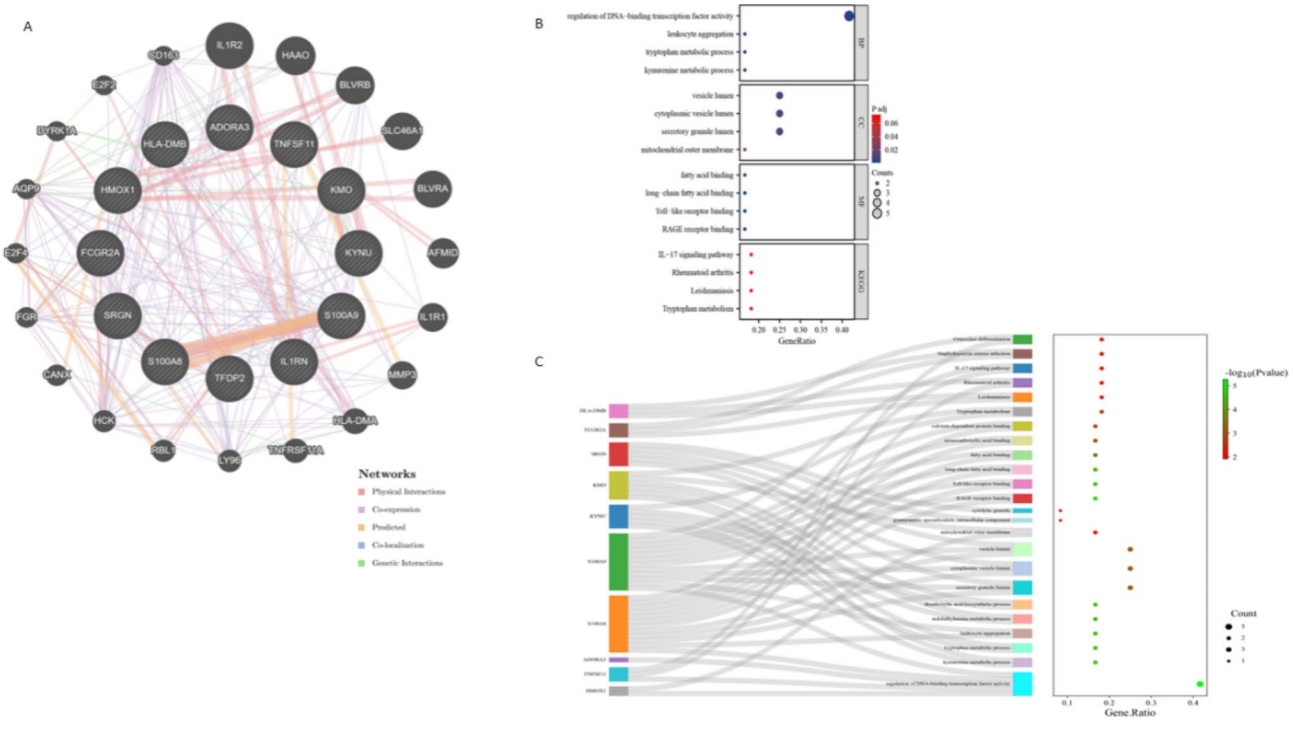

Fig. 3. Enrichment analysis of shared genes for both OP and AVC diseases. A. PPI network of 13 shared genes obtained by GeneMANIA construction. B, C. GO, KEGG enrichment analysis of 13 shared genes.

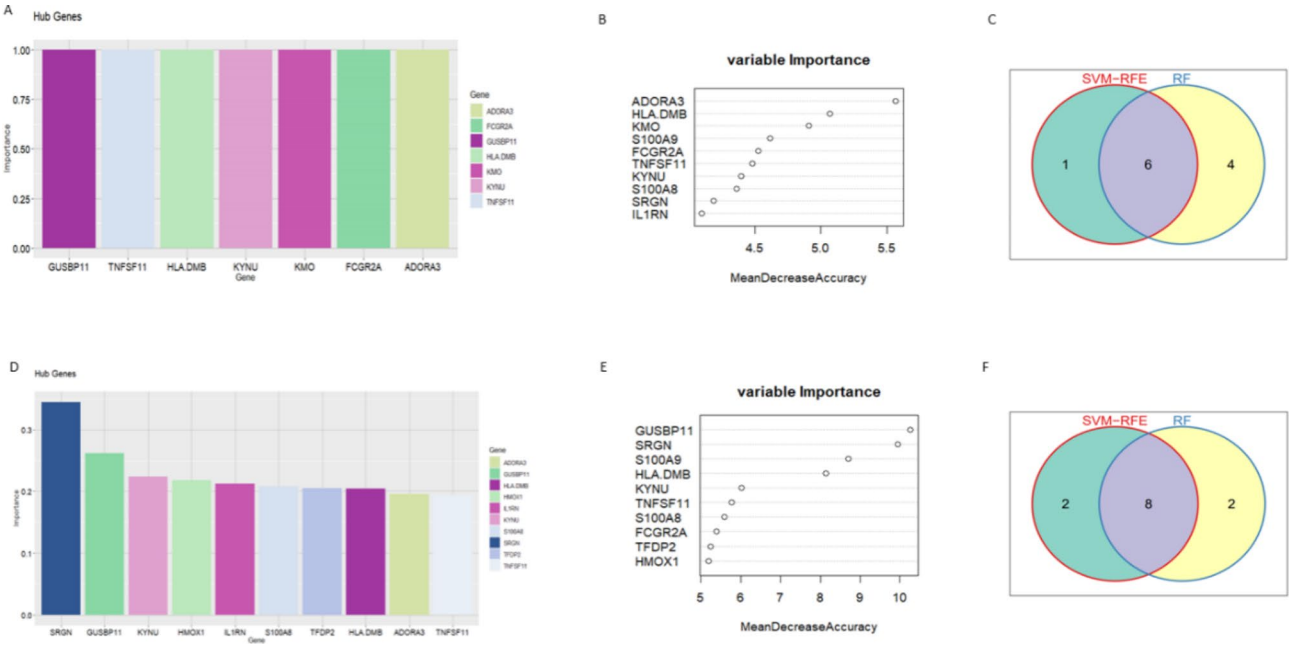

Fig. 4. Screening candidate diagnostic biomarkers for OP vs. AVC using machine learning. A, D. Screening biomarkers for AVC and OP using SVM-RFE algorithm, respectively. B, E. Importance of genes sorted by MeanDecreaseAccuracy value for screening biomarkers for AVC and OP using Randomized Survival Forest Algorithm. C. Wayne plots showing the importance of the AVC 6 genes common to both algorithms. F. Wayne diagram showing 8 genes common to both algorithms for OP.

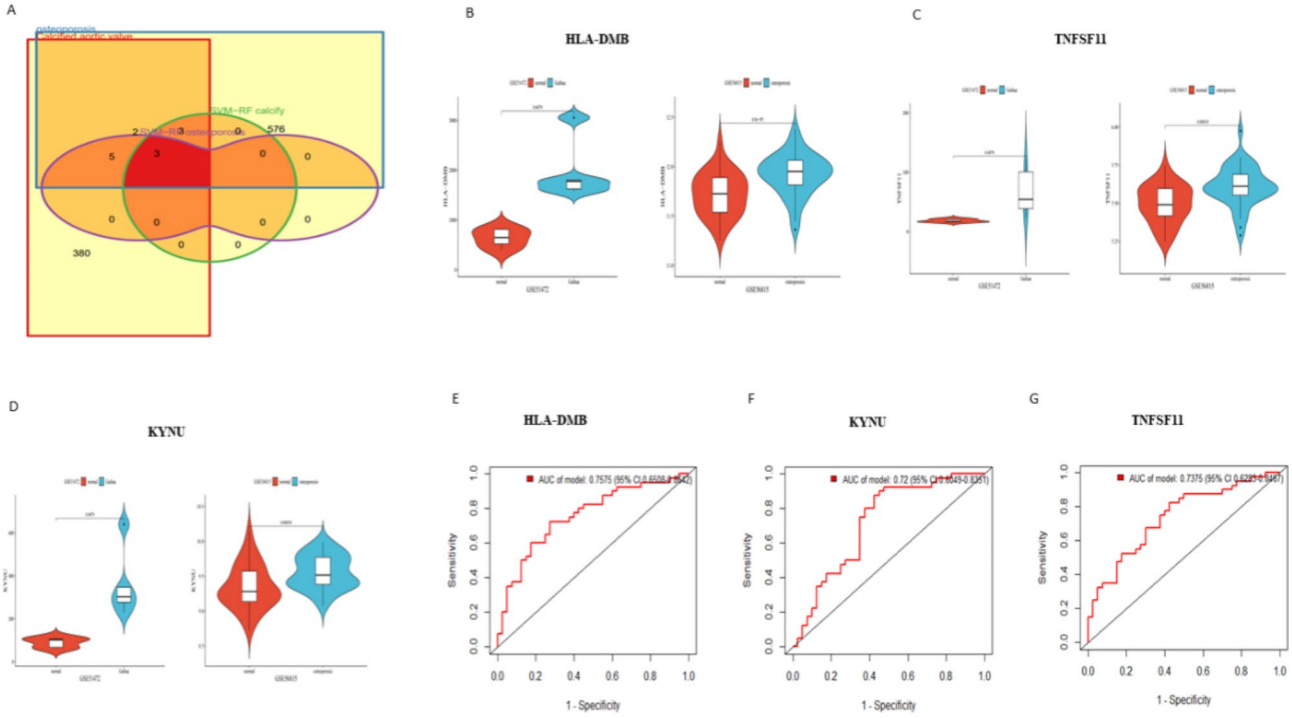

Fig. 5. Expression of common genes in the two diseases. (**A**) Wayne plots showing the three common genes obtained by two algorithms for the two diseases. (**B**) Expression level of HLA-DMB in the two diseases. (**C**) Expression level of TNFSF11 in the two diseases. (**D**) Expression level of KYNU in the two diseases. (**E, F, G**) The ROC curves of the three genes, namely, HLA-DMB, TNFSF11 and KYNU ROC curves of the three genes in the OP dataset.

three shared hub genes across both diseases. The results depicted in Fig. 5A and D revealed high expression levels of TNFSF11, KYNU, and HLA-DMB in both the AVC and OP cohorts. Subsequently, to evaluate the specificity and sensitivity of the three target genes for diagnosing the two conditions, Receiver Operating Characteristic (ROC) analysis was conducted. Regarding the AVC biomarker, all three genes exhibited an Area Under the Curve (AUC) value of 1.00 (indicating potential overfitting). Similarly, the ROC analysis was conducted for the OP cohort, demonstrating robust predictive capabilities for each biomarker: HLA-DMB (AUC = 0.7575), KYNU (AUC = 0.72), and TNFSF11 (AUC = 0.7375) (Fig. 5E-G).

Shared hub gene immune infiltration analysis

Considering that PCOS and RIF are characterized by high immune responses, the abundance of immune cells in the different groups was analyzed using CIBERSORT. In each group, the proportion of 22 immune cells is shown as a bar graph. In general, the bar graphs clearly illustrate the significant differences between the percentages of T cells, macrophages, and NK cell populations between AVC (Fig. 6A) and OP (Fig. 6D). According to Spearman correlation analysis, B cells naive was strongly negatively correlated with T cells CD4 memory resting, and T cells gamma delta was strongly negatively correlated with eosinophils in the AUC group (Fig. 6B). In the OP group, T cells regulatory (Tregs) showed a strong positive correlation with Macrophages M2. Macrophages M2 showed a strong positive correlation with B cells naïve, and T cells regulatory (Tregs) exhibited a strong negative correlation with B cells naïve (Fig. 6E). There was a significant decrease in T cells CD8 and an increase in B cells naïve in AVC compared with control samples (Fig. 6C). In contrast, macrophage M0 was increased in OP (Fig. 6F).

Biological functions and pathways of GSEA based on hub gene expression

Subsequently, we performed single-gene GSEA analyses of the three hub genes in the osteoporosis and AVC datasets, respectively, and visualised the top five up- and down-regulated pathways with the 'GSEA' package. In the osteoporosis disease group, HLA-DMB was only enriched for two down-regulated pathways, Focal adhesion and MicroRNAs in cancer (Fig. 7A), KYNU was only enriched for two up-regulated pathways, Phagosome and Tuberculosis (Fig. 7B), and TNFSF11 was enriched for other down-regulated pathways, Endocytosis and Salmonella infection. Salmonella infection among other down-regulated pathways (Fig. 7C). However, in the AVC disease group, all three genes were involved in the Ribosome metabolic pathway (Fig. 7D E F), and both HLA-DMB and TNFSF11 were involved in alpha-Linolenic acid metabolism, Ether lipid metabolism, Fat digestion and absorption, and Linolenic acid metabolism. Absorption and Linoleic acid metabolism (Fig. 7D F).

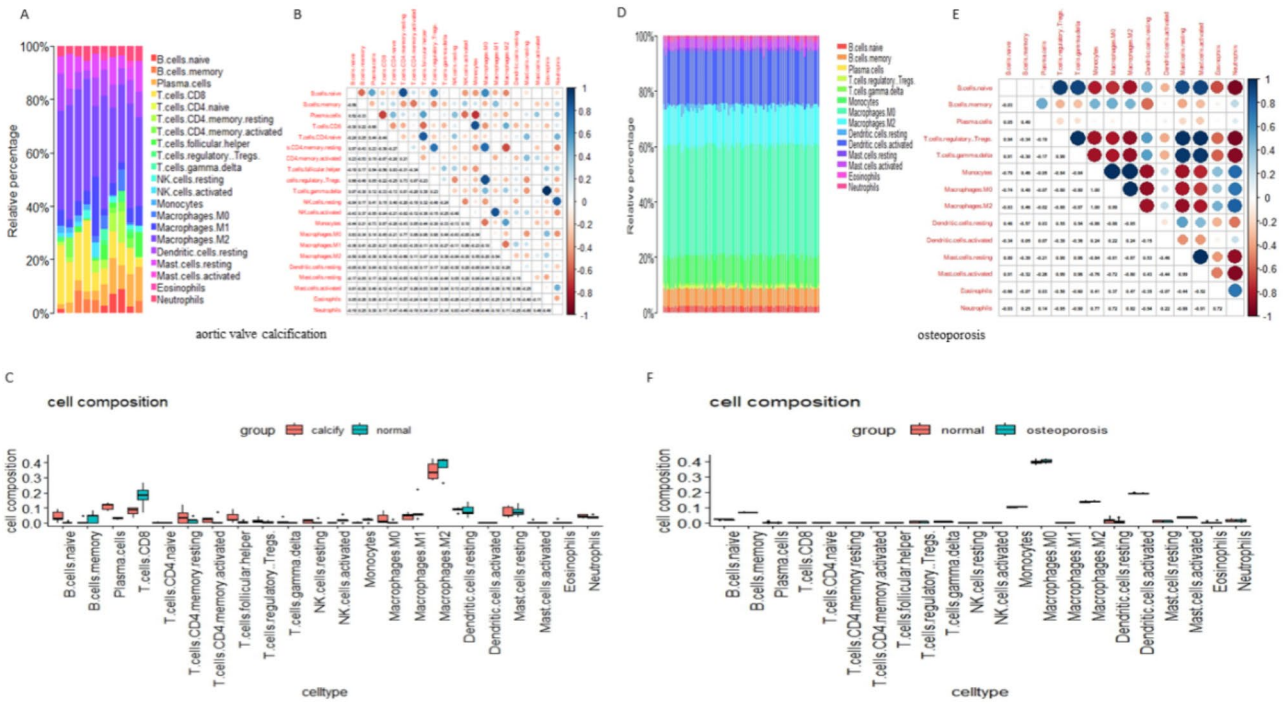

Fig. 6. Composition of immune cells in OP and AVC. (**A**) Infiltrating immune cells in the AVC group are plotted as stacked bars. (**B**) Heat map of correlation between immune cells in the AVC group. (**C**) Box line diagram of immune cell composition in the AVC group. (**D**) Infiltrating immune cells in the OP group are plotted as stacked bars. (**E**) Heat map of correlation between immune cells in the OP group. (**F**) Box line diagram of immune cell composition in the OP group. line diagram.

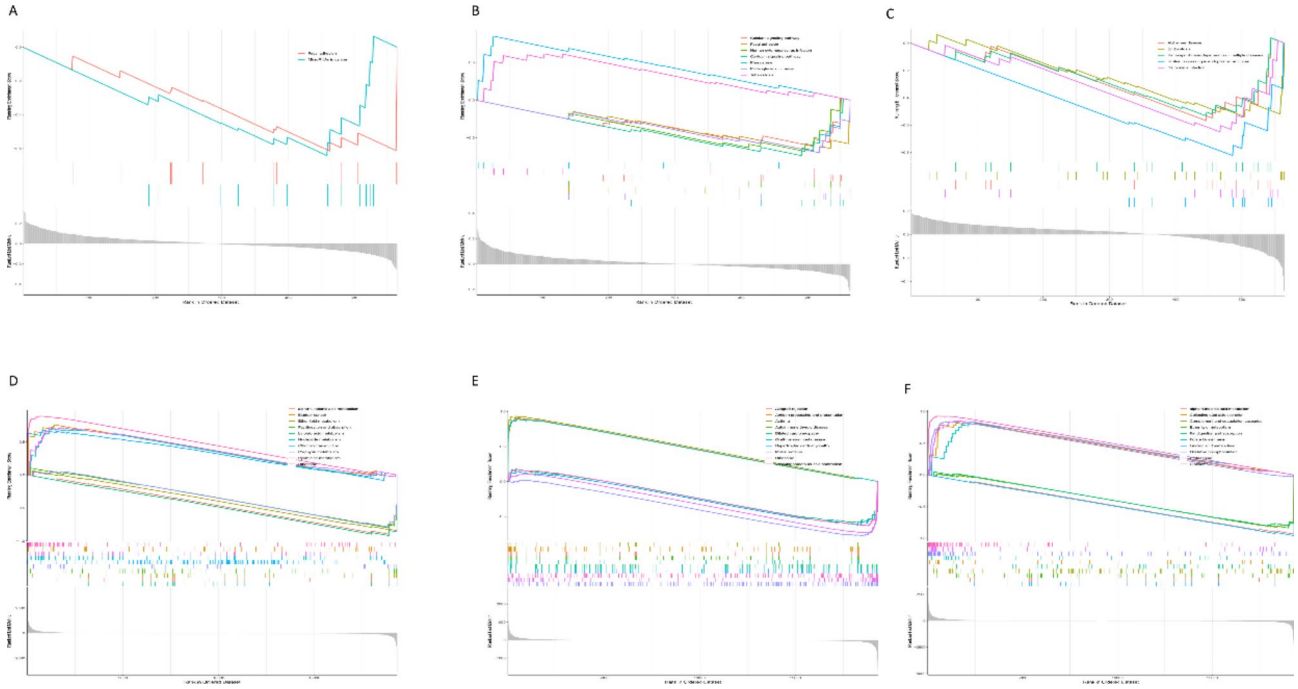

Fig. 7. GSEA of the expression levels of three genes, HLA-DMB, TNFSF11 and KYNU, in the OP dataset. (**A, B**) KEGG analysis by GSEA. (**C**) GO: BP analysis by GSEA. (**D**) GO: MF analysis by GSEA. (**E**) GO: CC analysis by GSEA. (**F**) Reactome pathway analysis by GSE. (**A**) Reactome pathway analysis. (**G**) Demonstration of GSEA enrichment results by ridge diagram.

Hub gene miRNA, TF, and small molecule drug analysis

Prediction of the three hub genes revealed that only KYNU was associated with 27 relevant miRNAs (Fig. 8A). The analysis of transcription factors led to the discovery of 17 TFs that regulate the hub genes (Fig. 8B). Subsequently, a small molecule drug prediction analysis was conducted on the three hub genes, revealing that only KYNU and TNFSF11 were associated with relevant small molecule drugs, resulting in the prediction of 40 small molecule drugs in total (Fig. 8C).

Molecular docking

Two genes, KYNU and TNFSF11, each linked to a specific small molecule drug, such as 17-beta-estradiol and vitamin D3, were chosen for molecular docking visualization, respectively (Fig. 9). In Fig. 9A, a robust binding energy is observed between vitamin D3 and TNFSF11, resulting in the formation of 1 hydrogen bond and involving the amino acid ARG-39. Figure 9B illustrates a significant binding energy between 17-beta-estradiol and KYNU, forming 2 hydrogen bonds at specific docking positions, namely the 1st and 38th amino acids, which are ARG-313 and MET-316, respectively.

Discussion

Both OP and AVC are highly prevalent diseases that often co-occur, carrying significant public health implications[35]. Hence, it is crucial to investigate the shared pathogenesis and biomarkers of these conditions. This study identifies common gene clusters significantly associated with both OP and AVC. In addition, functional analyses using GO and KEGG revealed a number of biological processes and pathways, which led to the identification of potential modes of action. The results from the GO analysis indicated that gene compositions primarily concentrated on leukocyte aggregation, binding to the RAGE receptor, and the mitochondrial outer membrane. This suggests that a significant number of these genes are engaged in metabolic processes and inflammation. For instance, OP is linked to the processes of protein glycosylation and oxidative stress. Glycosylation reactions result in the formation of advanced glycation end-products (AGEs), which accumulate in bone tissue and interact with the AGE receptor (RAGE)[36]. The RAGE receptor is part of the immunoglobulin superfamily of cell-surface proteins expressed in various cell types, such as osteoblasts and osteoclasts. When AGEs bind to RAGE, they enhance osteoclast activity while reducing osteoblast function[37], thus promoting bone resorption and contributing to bone fragility[38,39]. It is well established that the AGE/RAGE pathway plays a role in vascularization by facilitating phenotypic changes in vascular smooth muscle cells (VSMCs) in response to calcification associated with osteoblast-like cells[40]. Additionally, RAGE's downstream signaling mechanisms lead to the calcification of vascular mesenchymal cells through multiple pathways[41]. These genes exhibited notable enrichment in KEGG signaling pathways, particularly the IL-17 signaling pathway, Rheumatoid arthritis, Leishmaniasis, and Tryptophan metabolism, re-emphasizing that most of these shared genes are involved in immune and inflammatory pathways. For example, it has been shown that IL-17 promotes osteoclast-induced

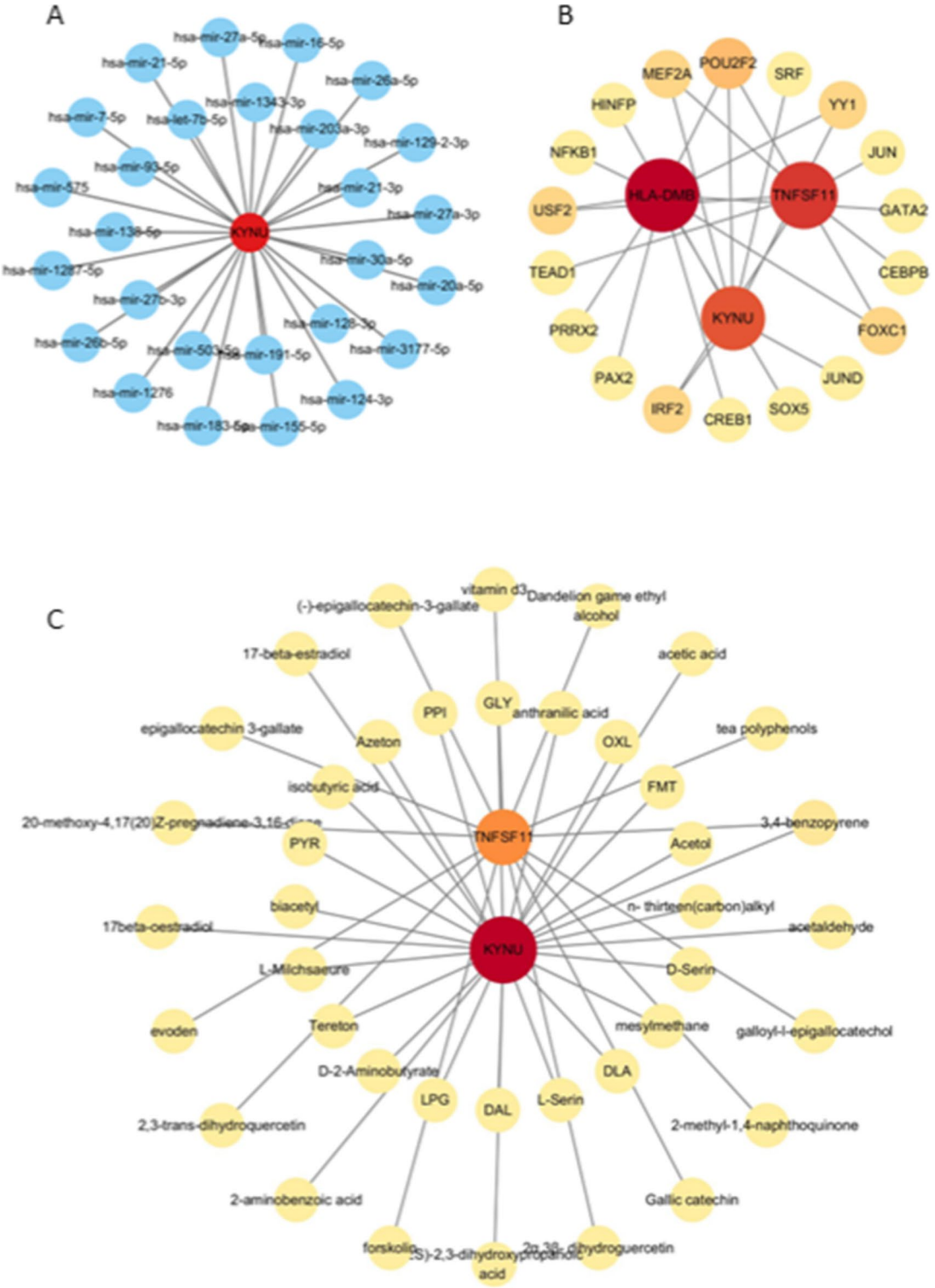

Fig. 8. Network diagram of common genes miRNA, TF and small molecule drug prediction. (**A**) Network diagram of common gene KYNU with miRNA. (**B**) Network diagram of common genes HLA-DMB, TNFSF11 and KYNU with TF. (**C**) Network diagram of two genes, TNFSF11 and KYNU, with small molecule drugs.

bone loss by regulating glutamine-dependent energy metabolism[42] and that IL-17 mediates estrogen-deficient OP in an Act1-dependent manner[43]. Elevated IL-17 A in calcific aortic valvulopathy promotes valvular inflammation, fibrosis, and calcification, possibly by inducing endothelial activation and inflammation[44], and IL-17 A promotes vascular calcification in isolated mouse aortic cultures[45].

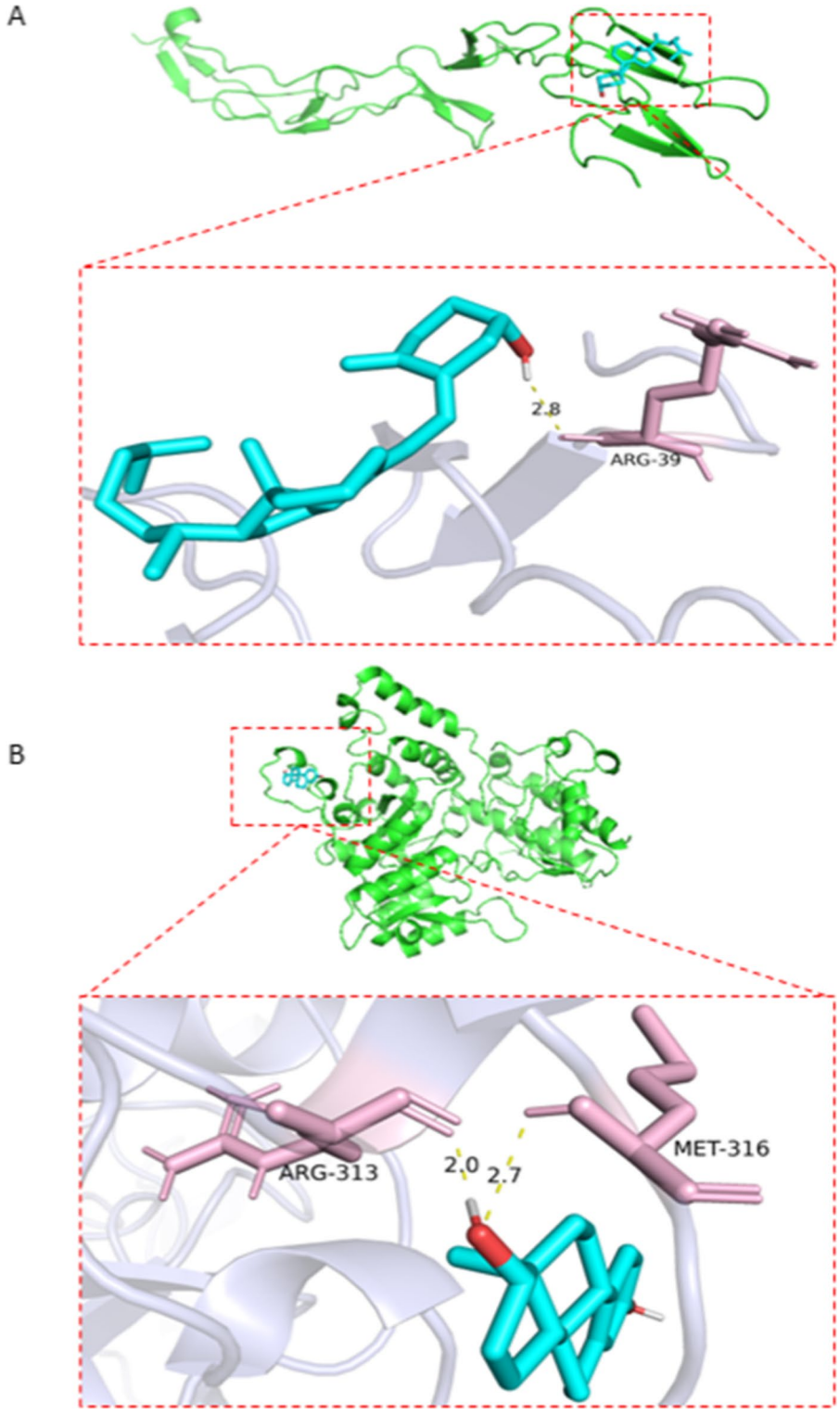

Fig. 9. A. Molecular docking of TNFSF11 with vitamin D3 and KYNU with 17-beta-estradiol visualised. (**A**) Molecular docking of TNFSF11 with vitamin D3 visualised, producing 1 hydrogen bond, this amino acid is ARG-39. (**B**) Molecular docking of KYNU with 17-beta-estradiol visualised to produce 2 hydrogen bonds, ARG-313 and MET-316.

Employing various algorithms, including Random Forest (RF) and SVM Recursive Feature Elimination (SVM-RFE). Regarding this similar approach to gene selection, previous studies have been reported by researchers who identified stage-specific genes in oral squamous cell carcinoma by logistic regression modeling[46], and by scholars who used penalized logarithmic net regular logistic regression modeling (logsum-NL) on top

of logistic regression modeling[47], Liu et al. similarly proposed a structured penalized logistic regression model that performs both feature selection and model learning for gene expression data analysis[48]. Considering the suitability of the samples of our selected dataset for this write-up, we therefore chose the RF and SVM-RFE algorithms that are more compatible with the sample size. These two algorithms allow for a comprehensive assessment of 13 candidate biomarkers. Comparative analysis of the algorithm results revealed three potential biomarkers—TNFSF11, KYNU, and HLA-DMB—identified as common biomarkers for both OP and AVC. Subsequent examination of the gene expression profiles in the patient cohort demonstrated markedly elevated expression levels of TNFSF11, KYNU, and HLA-DMB in both the OP and AVC cohorts compared to the control group. And this was confirmed by the analysis of the OP dataset, suggesting that TNFSF11, KYNU and HLA-DMB may serve as diagnostic biomarkers for OP in patients with AVC. This potential was corroborated by ROC analysis, demonstrating the highest accuracy across various datasets.

Tumor Necrosis Factor Ligand Superfamily Member 11 (TNFSF11), commonly referred to as RANKL[49]. S Previous studies have shown a correlation between TNFSF11 and OP[50], particularly highlighting genetic links and epigenetic modifications in the TNFSF11 gene (RANKL)[51]. Heightened expression of the Receptor Activator of Nuclear Factor κ-B Ligand (RANKL) in postmenopausal women significantly contributes to the pathogenesis of OP[52]. The interaction between RANKL and its corresponding receptor (RANK) initiates a series of signal transduction cascades, thereby stimulating osteoclast differentiation, activity, and viability[53]. Moreover, in senile OP cases with hip fractures, the expression of the TNFSF11 gene encoding the RANKL protein was elevated compared to that of osteoprotegerin protein[54]. Additionally, a correlation exists between TNFSF11 and AVC. A study indicated increased RANKL expression in AVC patients, showing a direct correlation with the extent of valve calcification[55]. In cultured human aortic valve myofibroblasts, RANKL promotes matrix calcification and induces the expression of osteoblast-associated genes, suggesting a shift to an osteogenic phenotype[56]. These findings imply an association of TNFSF11 (RANKL) with AVC. Our study proposes TNFSF11 as a promising diagnostic marker for individuals with OP and AVC, with some support from prior research.

KYNU is a pyridoxal phosphate (PLP)-dependent enzyme involved in the biosynthesis of tryptophan NAD cofactors[57]. Currently, studies on the KYNU gene have primarily focused on oncological contexts[58,59]. While the direct relationship between KYNU and AVC and OP remains unestablished, several studies have indicated that KYNU potentially plays a role in the pathogenesis of these diseases. Notably, macrophages overexpressing KYNU drive the progression of gastric cancer through unique ligand-receptor pairs and transcription factors, correlating with a poor clinical phenotype in gastric cancer[58]. However, there is mounting evidence suggesting that macrophages play a role in coordinating the interaction between osteoblasts and osteoclasts through the secretion of various cytokines[60,61].OP is characterized by an imbalance between bone formation mediated by osteoblasts and bone resorption mediated by osteoclasts[62]. Furthermore, macrophages have been demonstrated to play a role in regulating valvular calcification[63,64]. These findings suggest that KYNU could potentially impact the progression of OP and AVC through the regulation of macrophages; however, the precise mechanisms require further investigation.

Similarly, while limited studies have addressed HLA-DMB in OP and AVC, an indirect association between HLA-DMB and these conditions persists. It is noteworthy that studies have demonstrated the ability of HLA-DMB to induce the accumulation of autophagosomes through its regulatory role and its interaction with ATG7, a key autophagy protein essential for classical autophagy, leading to increased acetylation[65]. Notably, autophagy has garnered attention as a promising target for both the prevention and treatment of OP[66]. Likewise, autophagy is upregulated in calcified tissues of patients with calcified aortic valve stenosis[67]. It is evident that autophagy exerts a regulatory influence on AVC; however, the concept of "the enemy is the friend" necessitates further elucidation. These provide new ideas for future studies: does HLA-DMB play a role in regulating autophagy in both OP and AVC diseases? Further validation is warranted.

To investigate the potential pathogenic links and mechanisms between OP and AVC, we conducted GSEA on three diagnostic genes within both disease categories. The GSEA findings indicated that genes associated with both OP and AVC were notably enriched in metabolic pathways. Specifically, all three genes displayed enrichment in phenylalanine metabolism, taurine and hypotaurine metabolism, and tyrosine metabolism. Additionally, these genes were found to be enriched in the IL-17 and NF-kB signaling pathways, among others. Notably, IL-17 signaling has been associated with bone loss primarily in scenarios of significant inflammation, and inhibiting IL-17 signaling has been shown to mitigate estrogen-deficient osteoporosis by reducing osteoclast-mediated bone resorption[43]. Recent studies have also indicated that IL-17 promotes osteoclast-induced bone degradation by affecting glutamine-dependent energy metabolism[42]. Conversely, the role of IL-17 in AVC has received less attention; one study reported increased levels of IL-17 A in calcific aortic valve disease, which may contribute to valve inflammation, fibrosis, and calcification by promoting endothelial activation and inflammation[44]. Further investigation into these specific mechanisms is warranted. This aligns with prior research highlighting the involvement of NF-kB in both conditions[68–71].

Immune cell activation leads to the production of inflammatory mediators, such as reactive oxygen species, pro-inflammatory cytokines, and chemokines, which directly influence bone metabolism and contribute to OP development[72]. Similarly, immune modulation and inflammatory regulation are prevalent across all stages of AVC[73]. Our study revealed that AVC patients exhibited elevated levels of CD8 T cells, plasma cells, CD4 memory activated T cells, and M0 macrophages, alongside reduced levels of naive B cells, CD4 resting T cells, activated NK cells, and M2 macrophages, aligning with previous research findings. Analysis of immune infiltration in OP demonstrated a strong positive correlation between T cells regulatory (Tregs) and Macrophages M2, while Macrophages M2 exhibited a strong negative correlation with B cells naive. Consistent with our observations, immune dysregulation in OP and AVC leads to the activation of numerous immune cells. Therefore, comprehending the mechanisms driving these immune dysregulations could pave the way for the development of targeted diagnostic and therapeutic strategies for both AVC and OP.

Next, we constructed miRNA and TF networks for the three common genes to identify upstream and downstream targets for treating both OP and AVC. Among the common genes, only KYNU was associated with the prediction of the corresponding miRNA. Simultaneously, all three common genes predicted POU2F2, suggesting its potential role as a TF in the shared mechanisms of OP and AVC, despite the current lack of studies on POU2F2 in these conditions. Subsequent analysis involved predicting small molecule drugs for the common genes, with TNFSF11 and KYNU emerging as potential targets in our investigation. Based on these findings, we selected 17-beta-estradiol and vitamin D3 for molecular docking with KYNU and TNFSF11, respectively. Our study revealed strong binding energies between 17-beta-estradiol and vitamin D3 with KYNU and TNFSF11, indicating their potential as therapeutic targets for managing OP and AVC.17-beta-estradiol has been used in the treatment of a wide range of diseases including OP and AVC has been well documented[74,75]. Early research has indicated that 17-beta-estradiol enhances osteoblast differentiation and calcification in vascular cells[76] and that, in vitro, treatment with 17-beta-estradiol induces calcification in cultured vascular smooth muscle cells (VSMCs) by facilitating their differentiation into osteoblast-like cells[76,77]. Conversely, estrogen can also inhibit the differentiation of VSMCs into osteoblasts by inducing autophagy through the selective estrogen receptor alpha (Erα) signaling pathway, thereby reducing arterial calcification in vivo by enhancing autophagy[78] and maintain VSMCs in a contractile phenotype[79]. The varying effects of 17-beta-estradiol might depend on the timing of treatment, which is critical, as beneficial outcomes are observed when treatment begins early, prior to lesion development, but not when initiated after advanced lesions have formed[77,80]. It is widely recognized that 17-beta-estradiol is highly effective in treating osteoporosis (OP). Its anti-osteoporotic effects are mediated through the activation of the novel ESR1-Keap1-Nrf2 axis, which enhances the stress response and upregulates Tmem119[81]. Furthermore, low-dose micronized 17-beta-estradiol has been shown to prevent bone loss in postmenopausal women[82]. Thus, employing 17-beta-estradiol is notably significant when addressing the concurrent treatment of both conditions; however, the timing of administration is crucial for integrated and effective management. regarding vitamin D3 in the treatment of OP is indeed well documented[83], Whenever patients receive therapeutic drugs for osteoporosis, vitamin D supplementation is recommended to keep their calcium (Ca) balance positive[83]. In a prospective open-label randomized trial focused on osteoporosis, oral vitamin D3 regimens were found to enhance intestinal calcium absorption[84]. Nonetheless, the therapeutic implications of vitamin D3 for AVC require further investigation. Vitamin D deficiency has been identified as a risk factor for calcification in both aortic valves and vessels, as well as a trigger for the upregulation of key osteogenic factors in these vascular areas[85,86]. In the future, further studies should be conducted on the therapeutic efficacy of vitamin D3 in AVC, so as to find co-effective therapeutic agents.

Inherent limitations exist in this study, with the data obtained remaining limited. Further experimental biological studies and clinical trials are needed to assess the correlation of clinical parameters with hub genes. Elucidating the potential roles of TNFSF11, KYNU, and HLA-DMB in OP and AVC requires additional studies. Similarly, clarification of the exact mode of action of 17-beta-estradiol and vitamin D3 in OP and AVC treatment is necessary. The current research aims to offer a preliminary outlook on common biomarkers associated with OP and AVC, providing a crucial theoretical and empirical basis for the treatment of these diseases.

Conclusion

Our research has initially identified distinct biomarkers—TNFSF11, KYNU, and HLA-DMB—along with inflammatory responses that are common between OP and AVC, suggesting they may serve as potential susceptibility factors for both conditions. Importantly, our results indicated that 17-beta-estradiol and vitamin D3 exhibit strong binding affinities for KYNU and TNFSF11, respectively, highlighting their therapeutic potential and opening avenues for the development of novel treatment strategies. However, this study has certain limitations that must be addressed. Firstly, we utilized CIBERSORT for analyzing cellular composition, which, while informative, does not provide the cell type resolution that single-cell sequencing could offer. Secondly, although this study did not focus on genetic variability, it would be beneficial for subsequent research to utilize open-access Genome-Wide Association Study (GWAS) data, such as those from the UK Biospecimen Repository or the GTEx database, to investigate the associations between osteoporosis and single nucleotide polymorphisms (SNPs) linked to TNFSF11, KYNU, and HLA-DMB in the context of AVC. Finally, there is a need for more comprehensive validation through extensive animal and cellular studies. A significant focus for future research should be to overcome the limitations identified in this investigation.

Data availability

The datasets analysed during the current study can be found in the GEO repository [https://www.ncbi.nlm.nih.gov/geo/].

Received: 30 June 2024; Accepted: 4 November 2024
Published online: 13 November 2024

References

1. Driscoll, K., Cruz, A. D. & Butcher, J. T. Inflammatory and biomechanical drivers of endothelial-interstitial interactions in calcific aortic valve disease. *Circ. Res.* **128**, 1344–1370 (2021).
2. Cho, K. I., Sakuma, I., Sohn, I. S., Jo, S. H. & Koh, K. K. Inflammatory and metabolic mechanisms underlying the calcific aortic valve disease. *Atherosclerosis.* **277**, 60–65 (2018).
3. Lindman, B. R. et al. Calcific aortic stenosis. *Nat. Rev. Dis. Primers.* **2**, 16006 (2016).
4. Kanwar, A., Thaden, J. J. & Nkomo, V. T. Management of patients with aortic valve stenosis. *Mayo Clin. Proc.* **93**, 488–508 (2018).
5. Consensus development conference: Diagnosis, prophylaxis, and treatment of osteoporosis. *Am. J. Med.* **94**, 646–650 (1993).

6. Kasher, M. et al. Insights into the pleiotropic relationships between chronic back pain and inflammation-related musculoskeletal conditions: Rheumatoid arthritis and osteoporotic abnormalities. *Pain*. **164**, e122–e134 (2023).
7. Song, F. et al. Biomechanical CT-computed bone strength predicts the risk of subsequent vertebral fracture. *Bone*. **166**, 116601 (2023).
8. Wu, D., Li, L., Wen, Z. & Wang, G. Romosozumab in osteoporosis: Yesterday, today and tomorrow. *J. Transl Med*. **21**, 668 (2023).
9. Thompson, B. & Towler, D. A. Arterial calcification and bone physiology: role of the bone-vascular axis. *Nat. Rev. Endocrinol.* **8**, 529–543 (2012).
10. Prabhakaran, D. et al. Cardiovascular, respiratory, and related disorders: key messages from disease control priorities, 3rd edition. *Lancet* **391**, 1224–1236 (2018).
11. Lee, S. N., Cho, J. Y., Eun, Y. M., Song, S. W. & Moon, K. W. Associations between osteoporosis and coronary artery disease in postmenopausal women. *Climacteric*. **19**, 458–462 (2016).
12. Demer, L. L. Vascular calcification and osteoporosis: Inflammatory responses to oxidized lipids. *Int. J. Epidemiol.* **31**, 737–741 (2002).
13. Furugen, M. et al. Impact of osteogenic activity on degenerative aortic valve disease in patients with osteoporotic hip fracture. *J. Cardiol.* **78**, 423–430 (2021).
14. Lello, S., Capozzi, A. & Scambia, G. Osteoporosis and cardiovascular disease: An update. *Gynecol. Endocrinol.* **31**, 590–594 (2015).
15. Hjortnaes, J. et al. Arterial and aortic valve calcification inversely correlates with osteoporotic bone remodelling: A role for inflammation. *Eur. Heart J.* **31**, 1975–1984 (2010).
16. den Uyl, D., Nurmohamed, M. T., van Tuyl, L. H., Raterman, H. G. & Lems, W. F. (Sub)clinical cardiovascular disease is associated with increased bone loss and fracture risk; A systematic review of the association between cardiovascular disease and osteoporosis. *Arthritis Res. Ther.* **13**, R5 (2011).
17. Browner, W. S., Seeley, D. G., Vogt, T. M. & Cummings, S. R. Non-trauma mortality in elderly women with low bone mineral density. Study of Osteoporotic Fractures Research Group. *Lancet*. **338**, 355–358 (1991).
18. Lerner, U. H. Inflammation-induced bone remodeling in periodontal disease and the influence of post-menopausal osteoporosis. *J. Dent. Res*. **85**, 596–607 (2006).
19. Mishra, B. H. et al. Uncovering the shared lipidomic markers of subclinical osteoporosis-atherosclerosis comorbidity: The young finns study. *Bone*. **151**, 116030 (2021).
20. Demer, L. L. & Tintut, Y. Hearts of stone: Calcific aortic stenosis and antiresorptive agents for osteoporosis. *Circulation*. **143**, 2428–2430 (2021).
21. Chen, W. et al. Shared diagnostic genes and potential mechanism between PCOS and recurrent implantation failure revealed by integrated transcriptomic analysis and machine learning. *Front. Immunol.* **14**, 1175384 (2023).
22. Franz, M. et al. GeneMANIA update 2018. *Nucleic Acids Res.* **46**, W60–w64 (2018).
23. Yu, G., Wang, L-G., Han, Y. & He, Q-Y. clusterProfiler: An R package for comparing biological themes among gene clusters. *OMICS J. Integr. Biol.* **16**, 284–287 (2012).
24. Kanehisa, M., Sato, Y., Kawashima, M., Furumichi, M. & Tanabe, M. KEGG as a reference resource for gene and protein annotation. *Nucleic Acids Res.* **44**, D457–D462 (2016).
25. Shen, S., Wei, J., Kang, W. & Wang, T. Elucidating shared biomarkers and pathways in kidney stones and diabetes: Insights into novel therapeutic targets and the role of resveratrol. *J. Transl. Med.* **21** (2023).
26. Guan, M., Jiao, Y. & Zhou, L. Immune infiltration analysis with the CIBERSORT method in lung cancer. *Dis. Mark.* **2022**, 3186427 (2022).
27. Zhu, E. et al. Screening of immune-related secretory proteins linking chronic kidney disease with calcific aortic valve disease based on comprehensive bioinformatics analysis and machine learning. *J. Transl Med.* **21**, 359 (2023).
28. Liu, Z. et al. Identification of GLS as a cuproptosis-related diagnosis gene in acute myocardial infarction. *Front. Cardiovasc. Med.* **9**, 1016081 (2022).
29. Zhou, G. et al. NetworkAnalyst 3.0: A visual analytics platform for comprehensive gene expression profiling and meta-analysis. *Nucleic Acids Res.* **47**, W234–w241 (2019).
30. HM, B. et al. The Protein Data Bank. *Acta Crystallogr D Biol Crystallogr.* **58**(Pt 6 No 1), 899–907 (2002).
31. Sankar, K. et al. A descriptor set for quantitative structure-property relationship prediction in. *Mol. Inf.* **41** (9), e2100240. https://doi.org/10.1002/minf.202100240 (2022). Epub 2022 Mar:- e2100240.
32. GM, M. & MF, R. H. W. L. AutoDock4 and AutoDockTools4: automated docking with selective receptor. *-J. Comput. Chem.* **30** (16), 2785–2791. https://doi.org/10.1002/jcc.21256.:- (2009).
33. Id, S. K., Id, O. J. C. & Id, O. T. C. PubChem 2023 update. *Nucleic Acids Res.* **51** (D1), D1373–D1380. https://doi.org/10.1093/nar/gkac956 (2023).
34. NM, O. B., CA, M. B. & C, J. GR H - Open Babel: An open chemical toolbox. *J. Cheminform*. **3**, 33. https://doi.org/10.1186/1758-2946-3-33 (2011).
35. Aksoy, Y. et al. Aortic valve calcification: Association with bone mineral density and cardiovascular risk factors. *Coron. Artery Dis.* **16**, 379–383 (2005).
36. Schmidt, A. M., Yan, S. D., Yan, S. F. & Stern, D. M. The biology of the receptor for advanced glycation end products and its ligands. *Biochim. Biophys. Acta*. **1498**, 99–111 (2000).
37. Tanaka, K., Yamaguchi, T., Kaji, H., Kanazawa, I. & Sugimoto, T. Advanced glycation end products suppress osteoblastic differentiation of stromal cells by activating endoplasmic reticulum stress. *Biochem. Biophys. Res. Commun.* **438**, 463–467 (2013).
38. Galliera, E. et al. Evaluation of circulating sRAGE in osteoporosis according to BMI, adipokines and fracture risk: A pilot observational study. *Immun. Ageing*. **14**, 13 (2017).
39. Willett, T. L., Pasquale, J. & Grynpas, M. D. Collagen modifications in postmenopausal osteoporosis: advanced glycation endproducts may affect bone volume, structure and quality. *Curr. Osteoporos. Rep.* **12**, 329–337 (2014).
40. Son, M. et al. *Attenuating Effects of Pyrogallol-Phloroglucinol-6,6-Bieckol on Vascular Smooth Muscle Cell Phenotype Changes to Osteoblastic Cells and Vascular Calcification Induced by High Fat Diet*. Vol. 12 (Nutrients, 2020).
41. Liu, H. et al. Celastrol alleviates aortic valve calcification via inhibition of NADPH oxidase 2 in valvular interstitial cells. *JACC Basic. Transl Sci.* **5**, 35–49 (2020).
42. Peng, R. et al. IL-17 promotes osteoclast-induced bone loss by regulating glutamine-dependent energy metabolism. *Cell. Death Dis.* **15**, 111 (2024).
43. DeSelm, C. J. et al. IL-17 mediates estrogen-deficient osteoporosis in an Act1-dependent manner. *J. Cell. Biochem.* **113**, 2895–2902 (2012).
44. Yang, Z. et al. IL-17A induces valvular endothelial inflammation and aggravates calcific aortic valve disease. *Biochem. Biophys. Res. Commun.* **672**, 145–153 (2023).
45. Hiramatsu-Asano, S. et al. IL-17A promotes vascular calcification in an ex vivo murine aorta culture. *Biochem. Biophys. Res. Commun.* **604**, 83–87 (2022).
46. Randhawa, V. & Acharya, V. Integrated network analysis and logistic regression modeling identify stage-specific genes in oral squamous cell carcinoma. *BMC Med. Genomics*. **8**, 39 (2015).
47. Zhou, Z., Huang, H. & Liang, Y. Cancer classification and biomarker selection via a penalized logsum network-based logistic regression model. *Technol. Health Care*. **29**, 287–295 (2021).

48. Liu, C. & Wong, H. S. Structured penalized logistic regression for gene selection in gene expression data analysis. *IEEE/ACM Trans. Comput. Biol. Bioinform.* **16**, 312–321 (2019).
49. Qin, Y. et al. Type II taste cells participate in mucosal immune surveillance. *PLoS Biol.* **21**, e3001647 (2023).
50. Techapatiphandee, M., Tammachote, N., Tammachote, R., Wongkularb, A. & Yanatatsaneejit, P. VDR and TNFSF11 polymorphisms are associated with osteoporosis in Thai patients. *Biomed. Rep.* **9**, 350–356 (2018).
51. Bouzid, A. et al. Genetic association of rs1021188 and DNA methylation signatures of TNFSF11 in the risk of conductive hearing loss. *Front. Med. (Lausanne)*. **9**, 870244 (2022).
52. Eghbali-Fatourechi, G. et al. Role of RANK ligand in mediating increased bone resorption in early postmenopausal women. *J. Clin. Invest.* **111**, 1221–1230 (2003).
53. Lacey, D. L. et al. Bench to bedside: Elucidation of the OPG-RANK-RANKL pathway and the development of denosumab. *Nat. Rev. Drug Discov.* **11**, 401–419 (2012).
54. Mencej, S., Prezelj, J., Kocijancic, A., Ostanek, B. & Marc, J. Association of TNFSF11 gene promoter polymorphisms with bone mineral density in postmenopausal women. *Maturitas*. **55**, 219–226 (2006).
55. Rattazzi, M. et al. RANKL expression is increased in circulating mononuclear cells of patients with calcific aortic stenosis. *J. Cardiovasc. Transl Res.* **11**, 329–338 (2018).
56. Kaden, J. J. et al. Receptor activator of nuclear factor kappaB ligand and osteoprotegerin regulate aortic valve calcification. *J. Mol. Cell. Cardiol.* **36**, 57–66 (2004).
57. Al-Mansoob, M., Gupta, I., Stefan Rusyniak, R. & Ouhtit, A. KYNU, a novel potential target that underpins CD44-promoted breast tumour cell invasion. *J. Cell. Mol. Med.* **25**, 2309–2314 (2021).
58. Shen, K., Chen, B., Yang, L. & Gao, W. KYNU as a biomarker of tumor-associated macrophages and correlates with immunosuppressive microenvironment and poor prognosis in gastric cancer. *Int. J. Genomics* **2023**, 4662480 (2023).
59. León-Letelier, R. A. et al. Kynureninase upregulation is a prominent feature of NFR2-activated cancers and is associated with tumor immunosuppression and poor prognosis. *Cancers (Basel)* **15** (2023).
60. Yang, D. H. & Yang, M. Y. The role of macrophage in the pathogenesis of osteoporosis. *Int. J. Mol. Sci.* **20** (2019).
61. Muñoz, J., Akhavan, N. S., Mullins, A. P. & Arjmandi, B. H. *Macrophage Polarization and Osteoporosis: A Review*12 (Nutrients, 2020).
62. Aibar-Almazán, A. et al. Current status of the diagnosis and management of osteoporosis. *Int. J. Mol. Sci.* **23** (2022).
63. Raddatz, M. A. et al. Macrophages promote aortic valve cell calcification and alter STAT3 splicing. *Arterioscler. Thromb. Vasc Biol.* **40**, e153–e165 (2020).
64. Lu, J., Xie, S., Deng, Y., Xie, X. & Liu, Y. Blocking the NLRP3 inflammasome reduces osteogenic calcification and M1 macrophage polarization in a mouse model of calcified aortic valve stenosis. *Atherosclerosis*. **347**, 28–38 (2022).
65. Wang, J. et al. HLA-DMB restricts human T-cell leukemia virus type-1 (HTLV-1) protein expression via regulation of ATG7 acetylation. *Sci. Rep.* **7**, 14416 (2017).
66. Li, X. et al. Targeting autophagy in osteoporosis: From pathophysiology to potential therapy. *Ageing Res. Rev.* **62**, 101098 (2020).
67. Carracedo, M. et al. Upregulated autophagy in calcific aortic valve stenosis confers protection of valvular interstitial cells. *Int. J. Mol. Sci.* **20** (2019).
68. Geng, B. et al. Platelet membrane-coated alterbrassicene a nanoparticle inhibits calcification of the aortic valve by suppressing phosphorylation P65 NF-κB. *Theranostics*. **13**, 3781–3793 (2023).
69. Wang, Y. et al. Dihydrotanshinone I inhibits aortic valve interstitial cell calcification via the SMAD1/5/8/NF-κB/ERK pathway. *Biomed. Pharmacother.* **139**, 111674 (2021).
70. Li, Y. et al. Urolithin B suppressed osteoclast activation and reduced bone loss of osteoporosis via inhibiting ERK/NF-κB pathway. *Cell. Prolif.* **55**, e13291 (2022).
71. Tao, H. et al. Urolithin A suppresses RANKL-induced osteoclastogenesis and postmenopausal osteoporosis by, suppresses inflammation and downstream NF-κB activated pyroptosis pathways. *Pharmacol. Res.* **174**, 105967 (2021).
72. Cline-Smith, A. et al. Ovariectomy activates chronic low-grade inflammation mediated by memory T cells, which promotes osteoporosis in mice. *J. Bone Min. Res.* **35**, 1174–1187 (2020).
73. Zhou, Y. et al. Identification of immune-associated genes in diagnosing aortic valve calcification with metabolic syndrome by integrated bioinformatics analysis and machine learning. *Front. Immunol.* **13**, 937886 (2022).
74. Matilla, L. et al. Sex-related signaling of aldosterone/mineralocorticoid receptor pathway in calcific aortic stenosis. *Hypertension*. **79**, 1724–1737 (2022).
75. Ettinger, B. Use of low-dosage 17 beta-estradiol for the prevention of osteoporosis. *Clin. Ther.* **15**, 950–962 (1993). discussion 949.
76. Balica, M., Boström, K., Shin, V., Tillisch, K. & Demer, L. L. Calcifying subpopulation of bovine aortic smooth muscle cells is responsive to 17 beta-estradiol. *Circulation*. **95**, 1954–1960 (1997).
77. McRobb, L. S. et al. Estrogen receptor control of atherosclerotic calcification and smooth muscle cell osteogenic differentiation. *Arterioscler. Thromb. Vasc Biol.* **37**, 1127–1137 (2017).
78. Peng, Y. Q. et al. Oestrogen inhibits arterial calcification by promoting autophagy. *Sci. Rep.* **7**, 3549 (2017).
79. Rzewuska-Lech, E., Jayachandran, M., Fitzpatrick, L. A. & Miller, V. M. Differential effects of 17beta-estradiol and raloxifene on VSMC phenotype and expression of osteoblast-associated proteins. *Am. J. Physiol. Endocrinol. Metab.* **289**, E105–112 (2005).
80. Hodis, H. N. et al. Vascular effects of early versus late postmenopausal treatment with estradiol. *N Engl. J. Med.* **374**, 1221–1231 (2016).
81. Yang, R. et al. 17β-estradiol plays the anti-osteoporosis role via a novel ESR1-Keap1-Nrf2 axis-mediated stress response activation and Tmem119 upregulation. *Free Radic Biol. Med.* **195**, 231–244 (2023).
82. Ettinger, B., Genant, H. K., Steiger, P. & Madvig, P. Low-dosage micronized 17 beta-estradiol prevents bone loss in postmenopausal women. *Am. J. Obstet. Gynecol.* **166**, 479–488 (1992).
83. Hagino, H. Vitamin D3 analogs for the treatment of osteoporosis. *Can. J. Physiol. Pharmacol.* **93**, 327–332 (2015).
84. Uenishi, K., Tokiwa, M., Kato, S. & Shiraki, M. Stimulation of intestinal calcium absorption by orally administrated vitamin D3 compounds: A prospective open-label randomized trial in osteoporosis. *Osteoporos. Int.* **29**, 723–732 (2018).
85. Schmidt, N. et al. Vitamin D receptor deficiency and low vitamin D diet stimulate aortic calcification and osteogenic key factor expression in mice. *PLoS One*. **7**, e35316 (2012).
86. Schmidt, N., Brandsch, C., Schutkowski, A., Hirche, F. & Stangl, G. I. Dietary vitamin D inadequacy accelerates calcification and osteoblast-like cell formation in the vascular system of LDL receptor knockout and wild-type mice. *J. Nutr.* **144**, 638–646 (2014).

Author contributions

JL S and HL contributed to the conception and design. JL S, YJ L and QP P: Writing-Original Draft, Visualization, Data curation, Formal analysis. JL S and HL: Conceptualization, Writing - Review & Editing, Supervision, Funding acquisition. All authors have read and approved the final manuscript.

Funding

This work was supported by National Natural Science Foundation of China (82301785), Sichuan Province Central Guiding Local Science and Technology Development Special Project (2023ZYD0072), Key research and

development projects of Sichuan Science and Technology Plan Project (2024YFFK0135) and Fujian Provincial Natural Science Foundation of China (2024J011450).

Declarations

Competing interests
The authors declare no competing interests.

Additional information
Correspondence and requests for materials should be addressed to J.S. or H.L.

Reprints and permissions information is available at www.nature.com/reprints.

Publisher's note Springer Nature remains neutral with regard to jurisdictional claims in published maps and institutional affiliations.